Journal of Membrane Science 476 (2015) 602–608

Contents lists available at ScienceDirect

Journal of Membrane Science

journal homepage: www.elsevier.com/locate/memsci

Thickness dependent effects of solubility and surface phenomena on the hydrogen transport properties of sputtered Pd77%Ag23% thin film membranes

Nicla Vicinanza [a], Ingeborg-Helene Svenum [a,c], Live Nova Næss [b], Thijs A. Peters [c], Rune Bredesen [c], Anne Borg [b], Hilde J. Venvik [a,*]

[a] Department of Chemical Engineering, Norwegian University of Science and Technology, NO-7491 Trondheim, Norway
[b] Department of Physics, Norwegian University of Science and Technology, NO-7491 Trondheim, Norway
[c] SINTEF Materials and Chemistry, 0314 Oslo, Norway

ARTICLE INFO

Article history:
Received 28 February 2014
Received in revised form
2 November 2014
Accepted 16 November 2014
Available online 24 November 2014

Keywords:
PdAg
Hydrogen
Solubility
Diffusivity
Topography

ABSTRACT

The hydrogen solubility and permeation in Pd77%Ag23% membranes have been determined as a function of temperature and membrane thickness. Unexpectedly, the solubility of hydrogen is found to systematically increase as the membrane thickness decreases from 11.2 to 2.2 μm. Topography studies by atomic force microscopy in conjunction with previously reported characterization suggest linkage of the hydrogen solubility to the density of grain boundaries. A higher average grain boundary density for thinner membranes results from the nucleation and growth proceeding during membrane fabrication by sputtering. For the membranes and conditions (no membrane pretreatment; 300–400 °C; $\Delta p_{H_2} \leq 200$ kPa) applied here, surface phenomena affect the hydrogen transport at thicknesses below ~5 μm. Determination of the solubility constants hence allowed the extraction of the bulk diffusivity parameters from the permeability measurements over the thicker membranes (6.7–11.2 μm), in good agreement with reported values obtained using other techniques.

1. Introduction

Palladium-based membranes are able to separate hydrogen from gaseous mixtures with high or perfect selectivity and high permeability [1]. However, pure Pd is subject to the α-to-β phase transition in the palladium–hydrogen system at $T < 300$ °C and $P < 2$ MPa, which causes the so-called hydrogen embrittlement. This is suppressed by alloying with other metals [2,3]. Alloying palladium with silver leads in addition to an increase of the hydrogen permeability [3–5], with a maximum permeability at approximately 23 wt% Ag [4].

Hydrogen permeation through a dense membrane generally follows the solution-diffusion mechanism, where Fick's law of diffusion describes the mass transport given by

$$J_{H_2} = \frac{p}{t}(p_1^n - p_2^n). \quad (1)$$

where P is the permeability of the membrane, t the thickness and p_1 and p_2 the partial pressure of hydrogen on the high and low pressure side of the membrane, respectively. The n-value is a number between 0.5 and 1, depending on the transport limiting step. The solution-diffusion mechanism defines the permeability (P) as the product of the diffusivity (D) and the solubility or Sieverts' constant (K) given by

$$P = DK \quad (2)$$

The diffusion of hydrogen is an activated process and the diffusivity is hence given by

$$D = D_0 \exp(-E_a/RT). \quad (3)$$

Here, D_0 is a pre-exponential factor, E_a is the activation energy for diffusion, T is the temperature and R is the gas constant.

The solubility of hydrogen in palladium (Pd) and Pd-based alloys can be described by Sieverts' law, where the concentration of atomic hydrogen in the metal is proportional to the square root of the hydrogen partial pressure at constant temperature [6]. Dilute solution of hydrogen in the metal and no interactions between hydrogen atoms are assumed. Burch and Francis [7] observed that deviations from Sieverts' law in pure palladium occur at temperatures lower than 250 °C and atomic ratios (H/Pd) of hydrogen to palladium above 0.006. According to Evans [8], Sieverts' law is not obeyed at high pressure (> 13.33 kPa) as the concentration of absorbed hydrogen in palladium increases. Validation of Sieverts' law has been shown at low hydrogen content [6,8–10]. Both the solubility and the diffusivity

* Corresponding author. Tel.: +47 73592831.
E-mail address: hilde.j.venvik@ntnu.com (H.J. Venvik).

http://dx.doi.org/10.1016/j.memsci.2014.11.031

of hydrogen in palladium depend on the temperature. While the diffusivity is enhanced by increasing temperature, the solubility decreases. Sieverts demonstrated that one volume of palladium is able to absorb up to 800 atmospheric volumes of hydrogen at 20 °C, while only 56 volumes at 140 °C [6]. The hydrogen solubility increases with silver content and reaches a maximum at 20–40% Ag [2,11–14], while the diffusion coefficient decreases [4,13,14]. The simultaneous changes in solubility and diffusivity lead to a value of permeability ~1.7 times higher for alloys with 23 wt% of Ag than for pure Pd at 350 °C [15,16]. Different measurement principles can be applied to determine hydrogen solubility in palladium and its alloys [17], of which volumetric [18–20] and gravimetric [21–23] absorption, sample dilation measurements [24] and electrical resistance measurements [25] are a few examples. Flanagan and Oates [26] reported a series of methods used to estimate diffusivity in the palladium–hydrogen system.

The permeation through PdAg membranes is hence a combined kinetic and thermodynamic property [13]. Given that thin, defect/pinhole-free membranes can be manufactured, the picture becomes further complicated at the point where surface phenomena affect the transport, and even more so if the thin Pd membrane is supported by a porous mechanical support material that may also impose transport limitations. The Pd-alloy membrane fabrication technique developed by SINTEF utilizing magnetron sputtering [27,28] has enabled membrane investigations with thicknesses down to 1 μm without defects, i.e. 100% selectivity, and in configurations where mass transfer limitations in the gas phase can be largely reduced [29–31]. We have previously presented results that indicate that the surface as well as the bulk microstructure and composition of the Pd77%Ag23% membranes affect the permeation, and that this may be affected by membrane treatment [32–35]. Previous investigations also indicate that – *depending on the conditions and the pre-treatment of the membrane* – surface limitations start to affect the permeation for thicknesses below ~5 μm [36–39]. The so-called heat treatment in air, essentially an oxidation–reduction cycle of the surface to a ~2 nm thick oxide [35], has been demonstrated to enhance the hydrogen transport kinetics [19,20,32–35,40–45] as well as to suppress the competitive adsorption of CO [44]. The findings have been linked to segregation phenomena [35,42,43,46] as well as roughening of the surface [19,32,35,47,48] and removal of surface impurities [5,42,43,49], but are not fully understood. However, the heat treatment in air is not expected to affect hydrogen solubility in Pd–Ag membranes [19,20].

The aim of this work is to further disentangle the interplay between the bulk solubility and diffusion and the surface phenomena in thin Pd77%Ag23% membranes, taking into account also structural properties. The solubility has been experimentally obtained as a function of temperature, and for different membrane thicknesses. Permeation measurements have been performed in a microchannel configuration with insignificant limitations to the mass transfer from the gas phase to the surface of the membrane [29–31]. When applied jointly with solubility and characterization data, this allows for an improved analysis of the phenomena affecting the hydrogen transport.

2. Materials and methods

2.1. Membranes and hydrogen permeation

Pd77%Ag23% thin films were prepared at SINTEF by a unique two-steps sputtering technique [27,28], to nominal thicknesses ranging from 2.2 to 10.0 μm. The resulting thicknesses of the samples were measured by white-light interferometry. The thin films were peeled off the Si substrate wafer applied during sputtering and sealed in a microchannel configuration made of a polished stainless steel feed housing with seven parallel channels, a stainless steel permeate housing, and a polished stainless steel plate [29]. The steel plate had apertures for gas flow corresponding to a total active surface area of 0.91 cm^2, determined by the feed housing geometry. The membrane growth side from the sputtering process was always placed facing the feed housing of the apparatus, while the side that faced the substrate always faced the permeate side. The permeation measurements were performed at 300, 350 and 400 °C. 300 °C was reached by ramping at 2 °C/min under nitrogen (purity 99.999%) flow on the feed side and argon (purity 99.999%) on the permeate. No sweep gas was used during hydrogen (purity 99.999%) permeation tests. The permeate side was kept at atmospheric pressure while a differential pressure was applied reaching a maximum of 200 kPa. Permeate flow was measured accurately by using a film flow meter. A Micro-GC (Agilent) was applied to check for potential failure/leakage by feeding N_2 and using Ar permeate sweep. No experiments or membranes indicative of N_2 leakage have been included in the results.

2.2. Characterization

Equilibrium sorption measurements were carried out using an ASAP 2020 Chemisorption Analyzer (Micromeritics Instrument Corporation). Prior to any sorption measurement, a degassing procedure was performed in order to clean the sample surfaces from unwanted species. Following heating under He and evacuation, volumetric hydrogen sorption measurements were performed applying hydrogen pressures from 0.02 to 90.7 kPa. Hydrogen was always introduced to the system at 300 °C. In every measurement a sample mass close to 0.1 g (Mettler Toledo XA204 Delta Range Analytical Balance) of the as-grown PdAg film peeled off the substrate was used. The sorption measurements were carried out twice for each sample at each temperature: 300, 350 and 400 °C. Samples with thicknesses in the range 2.2–11.2 μm were investigated. The weight of the membranes was carefully checked after each sorption experiment, since the degassing procedure can cause a reduction in the mass. This sample weight was used to calculate the adsorbed volume of hydrogen per mass unit.

Atomic force microscopy (AFM) imaging was carried out using a Bruker Multimode AFM instrument with a Veeco Multimode controller in tapping mode under atmospheric conditions. The surface topography was investigated for both the growth/feed side and the substrate/permeate side of as-grown samples. At least five areas at different locations on the surface for each sample were imaged. The first flattening order command, provided by the Nanoscope Software (Version 7.2, by Veeco), was performed in order to remove tilt and noise from all images. The surface topography was quantified by determining the root mean square roughness (Rq) from the recorded images.

3. Results and discussion

3.1. Hydrogen solubility

A representative example of the measured equilibrium hydrogen sorption isotherms is shown in Fig. 1 for the 6.9 μm thick membrane. Linear fitting including pressure points below ~200 $Pa^{0.5}$ only, where Sieverts' law is mainly valid [8], was performed to obtain Sieverts' constant from the data. As shown (Fig. 1), there is little deviation between the two consecutive isotherms taken at each temperature, indicating negligible contributions from irreversible adsorption. Sieverts' constants of the Pd77%Ag23% thin films as a function of the film thickness are shown in Fig. 2 for different temperatures. The solubility always decreases with increasing temperature and shows similar

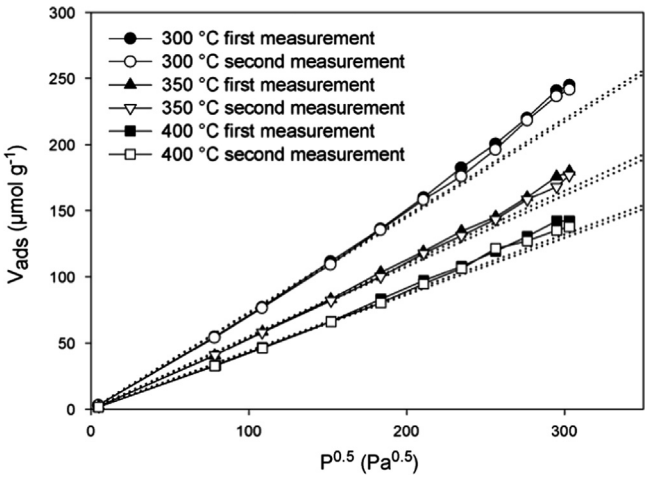

Fig. 1. Equilibrium hydrogen isotherms for a Pd77%Ag23% sample of 6.9 μm thickness. Experiments were done twice at each temperature of 300, 350 and 400 °C. Linear fits for the range up to 33.7 kPa are also shown (dotted lines).

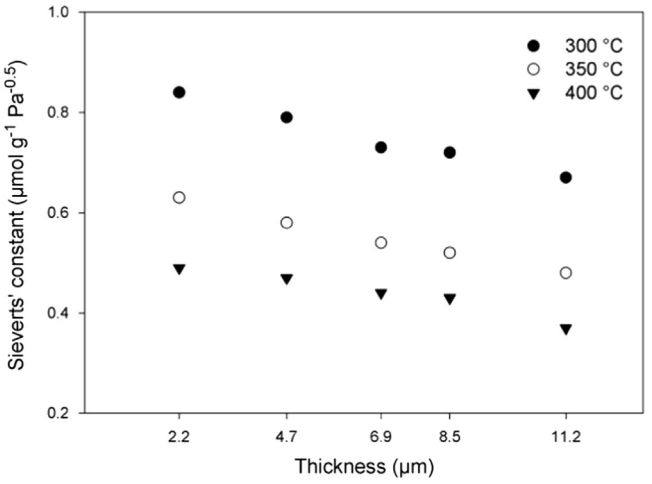

Fig. 2. Sieverts' constants as a function of the thickness of the Pd77%Ag23% thin film membranes for different temperatures.

temperature dependence for all membrane thicknesses. The difference in Sieverts' constant is always larger in the temperature range 300–350 °C than 350–400 °C, in accordance with the thermodynamic temperature dependency of the hydrogen solubility.

More unexpectedly, however, Fig. 2 shows that the hydrogen solubility consistently decreases with increasing membrane thickness. Solubility as an intrinsic material property should not depend on thickness, and the experiment was therefore repeated several times and with different samples. Although minor differences in Sieverts' constants were observed, the overall trend was always reproduced. Variations in hydrogen solubility in the Pd–Ag alloy membranes may be related to thickness dependent changes in the grain structure. Salomons et al. [21] attributed the enhancement of solubility in thin Pd-films to a strong influence of grain boundaries and increase of interface to volume ratio. The hydrogen uptake in palladium is also previously reported as dependent on the degree of crystallinity in the material [50–53]. Comparing nano-crystalline samples with average grain size 8–12 nm with polycrystalline Pd with average grain size of 20 μm, Mütschele and Kirchheim [51,52] found that the hydrogen solubility in palladium depended on the grain boundary density, but with opposite effects for the α (increase) and β phase (decrease). Not only grain boundaries can affect hydrogen solubility but also other lattice defects such as voids, vacancies, dislocations and impurity atoms. Flanagan et al. [54] suggested that deviations from Sieverts' law observed in their study could be attributed to hydrogen segregation in dislocations and vacancies. Moreover, going from the α to the β hydride phase (and vice versa) can also increase solubility [55], and this has been related to the large density of dislocations that the transformation generates [56,57]. The two-step sputtering technique used to obtain the Pd77% Ag23% membranes tested in this work avoids the presence of most potential contaminants, and analysis has confirmed the purity [27,28,34,35]. It is thus believed that impurities are not involved in the solubility variations found in the present work. Moreover, the composition (Pd–Ag) and experimental conditions applied have been chosen so as to avoid the phase transition. It has been established, however, that edge and screw dislocations are associated with the growth of the sputtered PgAg films, with twin lamellae present in the – mainly [111]-oriented – grains, but their dependency on grain size was not obtained [58]. Finally, it should be noted that our values for Sieverts' constant obtained for the 11.2 μm membranes compare reasonably well to values obtained for even thicker, typically cold-rolled, membranes [13,20,59]. The different reports are given for comparable, but not exactly similar, compositions and temperatures, and in addition there seem to be minor variations reflecting e.g. structural differences. Nevertheless, our values obtained for the thinnest membranes seem consistently 10–30% higher.

In an effort to link the grain structure of the Pd77%Ag23% thin films to the measured solubility, atomic force microscopy (AFM) imaging was used. The topography studies show an increase in the surface roughness on the growth side as the thickness increases for as-grown thin films (Fig. 3). The substrate side is very smooth and characterized by small grains, as reported in Table 1. Increased roughness on the growth side with growing membrane thickness has already been reported for sputtered membranes similar to those applied here [32,35]. Images of the substrate side were previously not reported in literature due to the resolution limitations imposed by the equipment available at the time [32,35]. This was possible with the current AFM, and an image representative of the substrate side for all the samples is shown in Fig. 3(a).

Surface roughness can be associated with grain size; the larger the grains present in the film, the rougher the surface [60]. In consistence, Tucho et al. [34] measured grain size variations in similar, sputtered Pd77%Ag23% films using X-ray diffraction (XRD) and transmission electron microscopy (TEM). The grain sizes measured by TEM were obtained from cross-section samples at about 0.1–0.2 μm below the surface. The region near the substrate was characterized by small grains around 12–18 nm. The region near the growth side had larger grains. The grains were larger for the 10 μm film compared to the 5 μm film, with average grain sizes of 100 [34] and 76 nm, respectively [61].

The grain structure of the sputtered films reflects the growth process. Under the sputtering conditions applied, the nucleation density on the Si wafer substrate is high, and the smooth nature of the wafer surface also affects the resulting roughness on the substrate side. As more material is deposited, some grains grow while others are terminated and covered. The result is a grain size gradient extending from the substrate interface into the film, with elongated grains of preferential orientation along the [111] direction. This is schematically illustrated in Fig. 4. As a result, the average grain size increases with the thickness while the average density of grain boundaries decreases. There may exist a thickness after which further grain growth does not occur, but the average values will be affected somewhat beyond this thickness.

3.2. Hydrogen transport kinetics

The permeabilities obtained from the flux measurements, assuming $n=0.5$, are given in Table 2. These are in good agreement with

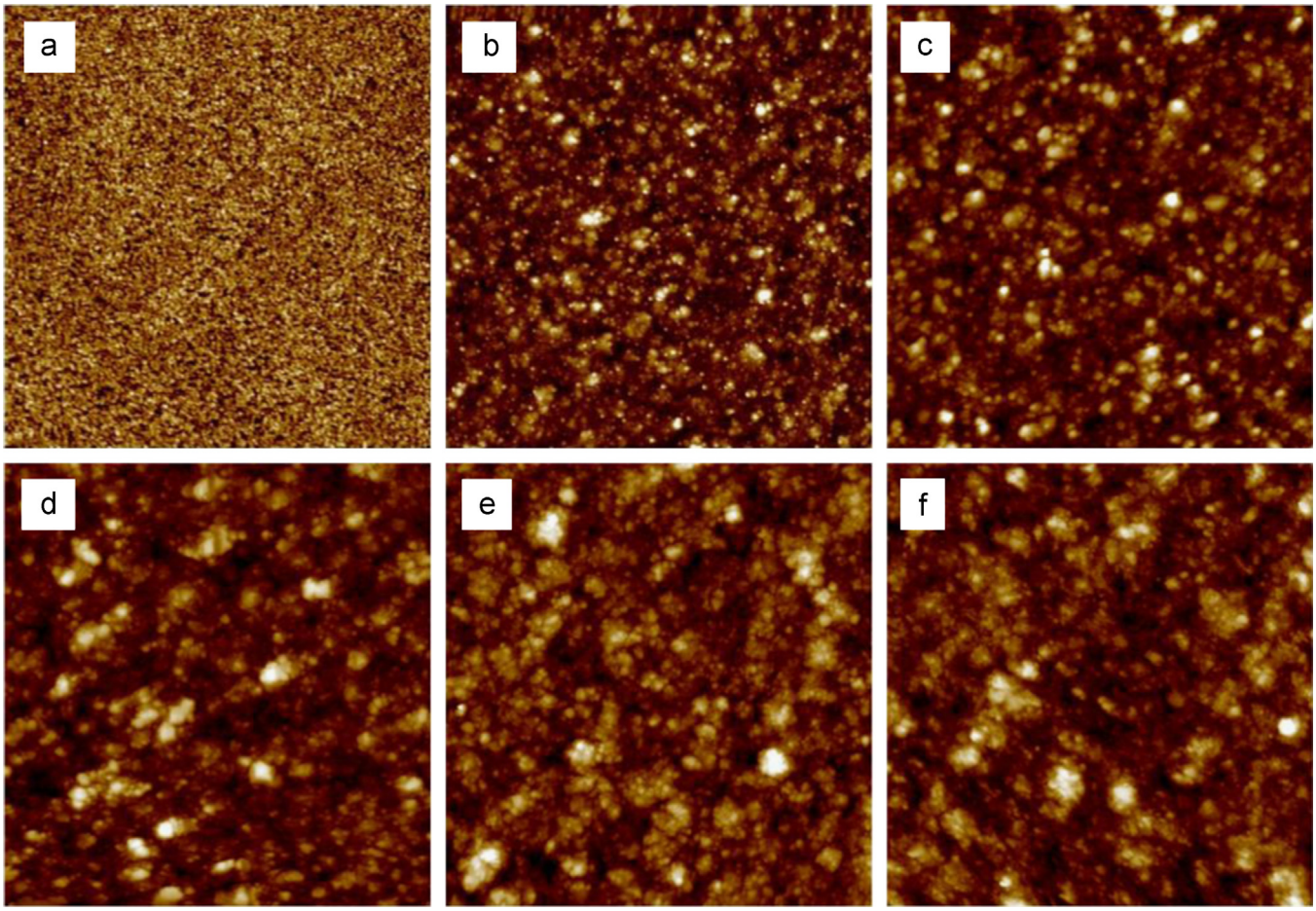

Fig. 3. Representative AFM topographic images as-grown Pd77%Ag23% films. (a) $1 \times 1\ \mu m^2$ scan area of the substrate/permeate side; (b)–(f) $5 \times 5\ \mu m^2$ scan areas from the growth/feed side of film thickness: (b) 2.2; (c) 4.7; (d) 6.9; (e) 8.5; and (f) 11.2 μm. (a) is obtained from the 2.2 μm thick sample, but representative of the substrate side of all thicknesses.

Table 1
Root mean surface roughness for the as-grown thin film membranes as obtained from analyzing the recorded AFM images.

Samples thickness (μm)	Roughness (nm)	
	Growth/feed[a]	Substrate/permeate[b]
2.2	8.4 ± 0.3	0.29 ± 0.02
4.7	10.7 ± 0.6	0.19 ± 0.01
6.9	11.8 ± 1.6	0.38 ± 0.04
8.5	10.2 ± 0.6	0.40 ± 0.03
11.2	13.2 ± 2.3	0.21 ± 0.01

[a] Based on $5 \times 5\ \mu m^2$ scan areas.
[b] Based on $1 \times 1\ \mu m^2$ scan areas.

Table 2
Permeabilities for the different Pd77%Ag23% thin film membranes as measured at 300, 350, and 400 °C.

Thickness (μm)	Permeability (10^{-8} mol m m^{-2} s^{-1} $Pa^{0.5}$)		
	300 °C	350 °C	400 °C
2.2	1.1	1.2	1.5
4.7	1.7	1.7	1.8
6.9	2.2	2.2	2.3
8.5	2.1	2.1	2.2
11.2	2.0	2.0	2.1

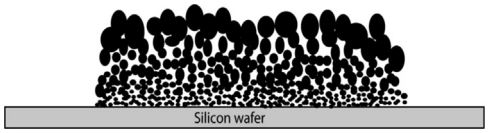

Fig. 4. Schematic illustration of the grain distribution of thin Pd–Ag films grown on silicon as resulting from the magnetron sputtering.

values obtained for similarly prepared Pd77%Ag23% membranes not subjected to oxidation under air at elevated temperature or other pretreatment [32,33,45]. Eqs. (1) and (2) were combined to analyze the effect of thickness and temperature on the kinetics. Fig. 5 shows the measured permeances (P/t, Eq. (1)) divided by the corresponding solubility (Sieverts) constants against the inverse thickness, applying a density of 11.674 g/cm^3 for Pd77%Ag23%. It shows that the diffusivity/thickness (P/Kt) systematically increases with temperature as expected. It also shows a reasonably linear dependence with $1/T$ for the thicknesses from 11.2 to 6.9 μm, indicating that bulk diffusion is controlling the transport. This is, however, not the case for the thinner membranes – with the leveling off of the values being a clear indication of surface phenomena becoming controlling. Through modeling, Ward and Dao predicted that hydrogen permeation through Pd membranes was bulk diffusion limited above ~573 K and membrane thicknesses down to about 1 μm, whereas desorption became the limiting process for lower temperatures and/or thicknesses [62]. As discussed in Section 1, previous experimental findings show that the critical thickness for the transition between surface and bulk limited transport also depends on the pretreatment and the conditions [33,35–39].

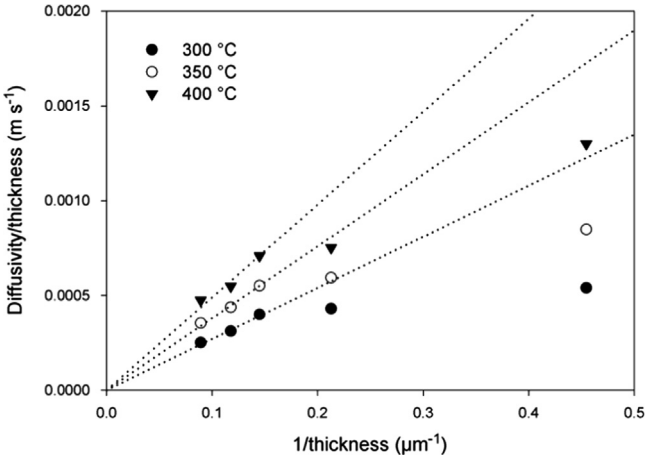

Fig. 5. Values of the permeance obtained at a differential pressure of 20 kPa under pure hydrogen divided by the solubility constant for the different Pd77%Ag23% membranes as function of inverse thickness for three different temperatures. The dotted lines suggest the linearity for the higher thicknesses.

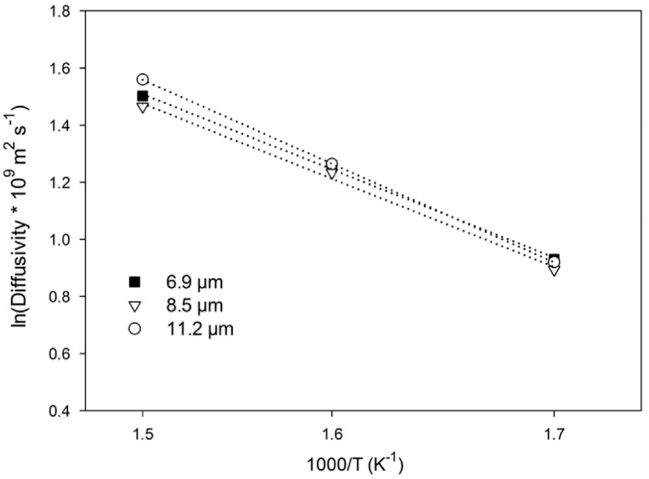

Fig. 6. Arrhenius plot of the diffusivity (logarithmic scale) in Pd77%Ag23% membranes of thickness $>5\,\mu m$ as function of inverse temperature. Linear fits are represented by dotted lines.

The applicability of Eqs. (1) and (2) must hence be considered, since, the flux can no longer be assumed proportional to the difference between the square root of the partial pressures, i.e. $n=0.5$ (1). In principle, surface kinetic control should be associated with $n=1$, but many investigations find n-values between 0.5 and 1, indicating that the transport mechanism is more complicated, see e.g. [63,64] and references cited therein. In addition, precise determination of the n-dependence by fitting of experimental data has been shown to require a wide differential pressure range [29,45]. The diffusivities calculated using Eq. (2) were therefore plotted as a function of inverse temperature to obtain the diffusivity constant and the activation energy according to Eq. (3)) for the three higher thicknesses only. The result is given in Fig. 6 and Table 3. D_0 in the range 1–2×10^{-7} m^2/s and $E_a\sim19$ kJ/mol are in good agreement with values of diffusivity reported by Holleck [13] for a thick (between 0.08 and 0.20 cm) Pd80%Ag20% membrane.

Whether the density of grain boundaries affect the diffusivity should be evaluated based on bulk-limited permeance data, i.e. in the thickness range $>5\,\mu m$ for the membranes and conditions applied here. If the above explanation on the thickness dependence of the solubility is adopted, our results indicate little or no effect of the grain boundary density on the transport. The literature is somewhat inconclusive with respect to the effect of grain boundaries and other lattice defects on the kinetics [51,65–67], likely reflecting the large microstructural variations possible in polycrystalline palladium and PdAg alloys. Mütschele and Kirchheim [51] reported values of the hydrogen diffusion coefficient in a single crystal Pd sample and in nano-crystalline Pd. The diffusivity of hydrogen in the Pd single crystal was independent of the hydrogen concentration. However, in the nano-crystalline Pd-sample, the hydrogen diffusivity changed with the hydrogen concentration in the material, i.e. increasing hydrogen pressure. Li and Cheng [69] attributed a decrease of the hydrogen diffusivity in very thin, pure Pd films relative to bulk Pd foil to lattice defects at grain boundaries. These experiments were conducted in a solution using electrochemical stripping at room temperature, and they also observed decreased solubility by electrochemical cycling. Comparing the present results to pure Pd investigations is complicated by the differences in phase behavior. The membrane micro- and nanostructures, as well as the purity and homogeneity of the alloy composition, are strongly affected by the membrane/film fabrication. In this respect, sputtering/evaporation, arc melting-cold rolling, and wet chemical techniques such as electroless plating are very different.

Table 3
Diffusivity pre-factor and activation barrier as obtained from linear fitting for the different Pd77%Ag23% thin film membranes of thickness $>5\,\mu m$.

Thickness (μm)	D_0 (m^2/s)	E_a (kJ/mol)
6.9	1.2×10^{-7}	18
8.5	1.2×10^{-7}	18
11.2	1.9×10^{-7}	21

The sputtering applied here results in pure and dense membranes of homogeneous bulk composition [68–70], highly suitable for detailed investigations of how the structure affects the membrane properties. The film nucleation and growth scheme produces, however, a gradient with respect to grain size across the thickness of the film. Systematic variation of thickness in the range 2.2–11 μm thus renders a variation in the average grain boundary density that possibly leads to variations in the thermodynamic properties. Careful solubility measurements were required to pick up this effect. The study envisages that such variations need to be addressed in order to increase the precision in transport kinetics analysis.

4. Conclusions

The solubility of hydrogen in sputtered Pd–Ag thin membranes shows an increase with decreasing membrane thickness. In addition, the hydrogen permeability exhibits variations with membrane thickness. This may be accounted for mainly by surface limitations when the thickness decreases below 5 μm, while the changes in permeability for the thicker membranes result from differences in hydrogen solubility rather than hydrogen diffusivity. The systematic variation in solubility may be related to gradients in grain size over the sputtered Pd–Ag thin films, with a larger fraction of smaller grains and higher average density of grain boundaries as the thickness is reduced.

Acknowledgment

The authors would like to acknowledge the financial support of the Research Council of Norway through the RENERGI Program (190779/S60) and CLIMIT Program (215666/E20), and NTNU, SINTEF and Statoil ASA through the Gas Technology Centre NTNU-SINTEF. Dr. M. Stange is also gratefully acknowledged for the manufacturing of the Pd-alloy

films, Prof. T. Tybell, I. Hallsteinsen and Dr. G. Maurstad is acknowledged for assisting with AFM experiments and Prof. R. Holmestad (NTNU) for providing previously unpublished data for grain size estimation in 5 μm Pd77%Ag23% membrane.

References

[1] F.A. Lewis, The palladium–hydrogen system, a survey of hydride formation and the effects of hydrogen contained within the metal lattices, Platin. Met. Rev. 26 (1982) 20–27.
[2] G.J. Grashoff, C.E. Pilkington, C.W. Corti, The purification of hydrogen – a review of the technology emphasising the current status of palladium membrane diffusion, Platin. Met. Rev 27 (1983) 157–169.
[3] A.K.M. Fazle Kibria, Y. Sakamoto, The effect of alloying of palladium with silver and rhodium on the hydrogen solubility, miscibility gap and hysteresis, Int. J. Hydrogen Energy 25 (2000) 853–859.
[4] S. Uemiya, T. Matsuda, E. Kikuchi, Hydrogen permeable palladium–silver alloy membrane supported on porous ceramicsr, J. Membr. Sci. 56 (1991) 315–325.
[5] N. Itoh, W.-C. Xu, Selective hydrogenation of phenol to cyclohexanone using palladium-based membranes as catalysts, Appl. Catal. A Gen. 107 (1993) 83–100.
[6] A. Sieverts, Die Aufnahme von Gasen durch Metalle, Z. Metallk. 21 (1929) 37–46.
[7] R. Burch, N.B. Francis, Pressure against composition isotherms and thermodynamic data for the α-phase of the palladium/hydrogen system, J. Chem. Soc. Faraday Trans. 1 (69) (1973) 1978–1982.
[8] M.J.B. Evans, Surface area effects on the sorption of hydrogen by palladium, Can. J. Chem. 52 (1974) 1200–1205.
[9] J.W. Simons, T.B. Flanagan, Absorption isotherms of hydrogen in the α-phase of the hydrogen–palladium system, J. Phys. Chem. A 69 (1965) 3773–3781.
[10] R. Lässer, G.L. Powell, Solubility of H, D, and T in Pd at low concentrations, Phys. Rev. B 34 (1986) 578–586.
[11] A. Sieverts, E. Jurisch, A. Metz, Die Löslichkeit des Wasserstoffs in den festen Legierungen des Palladiums mit Gold, Silber und Platin, Z. Anorg. Allg. Chem. 92 (1915) 329–362.
[12] A. Sieverts, H. Hagen, Der elektrische Widerstand wasserstoffbeladener Drahte aus Legierungen des Palladiums mit Silber und mit Gold, Z. Phys. Chem. 174A (1935) 247–261.
[13] G.L. Holleck, Diffusion and solubility of hydrogen in palladium and silver–palladium alloys, J. Phys. Chem. A 74 (1970) 503–511.
[14] Y. Sakamoto, S. Hirata, H. Nishikawa, Diffusivity and solubility of hydrogen in Pd–Ag and Pd–Au alloys, J. Less Common Met. 88 (1982) 387–395.
[15] D.L. McKinley, Metal alloy for hydrogen separation and purification, US Patent, 3,350,845, 1967.
[16] D.L. McKinley, Method for hydrogen separation and purification, US Patent, 3,439,474, 1969.
[17] F.D. Manchester, A. San-Martin, J.M. Pitre, The H–Pd (hydrogen–palladium) system, J. Phase Equilib. 15 (1994) 62–83.
[18] A. Sieverts, W. Krumbhaar, Über die Löslichkeit von Gasen in Metallen und Legierungen, Berichte Der Dtsch. Chem. Gesellschaft 43 (1910) 893–900.
[19] K. Zhang, S.K. Gade, Ø. Hatlevik, J.D. Way, A sorption rate hypothesis for the increase in H_2 permeability of palladium–silver (Pd–Ag) membranes caused by air oxidation, Int. J. Hydrogen Energy 37 (2012) 583–593.
[20] K. Zhang, S.K. Gade, J.D. Way, Effects of heat treatment in air on hydrogen sorption over Pd–Ag and Pd–Au membrane surfaces, J, Membr. Sci. 403–404 (2012) 78–83.
[21] E.M. Salomons, R. Feenstra, R. Griessen, D.G. De Groot, J.H. Rector, Pressure–composition isotherms of thin PdHc films, J. Less Common Met. 130 (1987) 415–420.
[22] M.J. Benham, D.K. Ross, Experimental determination of absorption-desorption isotherms by computer-controlled gravimetric analysis, Z. Phys. Chem. Neue Fol. 163 (1989) 25–32.
[23] D.T. Hughes, I.R. Harris, A comparative study of hydrogen permeabilities and solubilities in some palladium solid solution alloys, J. Less Common Met. 61 (1978) P9–P21.
[24] Y. De Ribaupierre, F.D. Manchester, Experimental study of the critical-point behaviour of the hydrogen in palladium system: I. Lattice gas aspects, J. Phys. C Solid State Phys. 7 (1974) 2126–2139.
[25] P. Wright, The effect of occluded hydrogen on the electrical resistance of palladium, Proc. Phys. Soc. A 63 (1950) 727–739.
[26] T.B. Flanagan, W.A. Oates, The palladium–hydrogen system, Annu. Rev. Mater. Sci. 21 (1991) 269–304.
[27] R. Bredesen, H. Klette, Method of manufacturing thin metal membranes, US Patent, 6,086,729, 2000.
[28] H. Klette, R. Bredesen, Sputtering of very thin palladium-alloy hydrogen separation membranes, Membr. Technol. 2005 (2005) 7–9.
[29] A.L. Mejdell, M. Jøndahl, T.A. Peters, R. Bredesen, H.J. Venvik, Experimental investigation of a microchannel membrane configuration with a 1.4 μm Pd/Ag23wt% membrane – effects of flow and pressure, J. Membr. Sci. 327 (2009) 6–10.
[30] A.L. Mejdell, T.A. Peters, M. Stange, H.J. Venvik, R. Bredesen, Performance and application of thin Pd-alloy hydrogen separation membranes in different configurations, J. Taiwan Inst. Chem. Eng. 40 (2009) 253–259.
[31] T. Boeltken, M. Belimov, P. Pfeifer, T.A. Peters, R. Bredesen, R. Dittmeyer, Fabrication and testing of a planar microstructured concept module with integrated palladium membranes, Chem. Eng. Process.: Process Intensif. 67 (2013) 136–147.
[32] A.L. Mejdell, H. Klette, A. Ramachandran, A. Borg, R. Bredesen, Hydrogen permeation of thin, free-standing Pd/Ag23% membranes before and after heat treatment in air, J. Membr. Sci. 307 (2008) 96–104.
[33] W.M. Tucho, H.J. Venvik, M. Stange, J.C. Walmsley, R. Holmestad, R. Bredesen, Effects of thermal activation on hydrogen permeation properties of thin, self-supported Pd/Ag membranes, Sep. Purif. Technol. 68 (2009) 403–410.
[34] W.M. Tucho, H.J. Venvik, J.C. Walmsley, M. Stange, A. Ramachandran, R.H. Mathiesen, et al., Microstructural studies of self-supported (1.5–10 μm) Pd/23 wt%Ag hydrogen separation membranes subjected to different heat treatments, J. Mater. Sci. 44 (2009) 4429–4442.
[35] A. Ramachandran, W.M. Tucho, A.L. Mejdell, M. Stange, H.J. Venvik, J.C. Walmsley, et al., Surface characterization of Pd/Ag23wt% membranes after different thermal treatments, Appl. Surf. Sci. 256 (2010) 6121–6132.
[36] A.L. Mejdell, Properties and application of 1–5 μm Pd/Ag23wt.% membranes for hydrogen separation, Nor. Univ. Sci. Technol. PhD thesis NTNU 76 (2009).
[37] B. McCool, G. Xomeritakis, Y. Lin, Composition control and hydrogen permeation characteristics of sputter deposited palladium–silver membranes, J. Membr. Sci. 161 (1999) 67–76.
[38] S.-E. Nam, S.-H. Lee, K.-H. Lee, Preparation of a palladium alloy composite membrane supported in a porous stainless steel by vacuum electrodeposition, J. Membr. Sci. 153 (1999) 163–173.
[39] L.-Q. Wu, N. Xu, J. Shi, Novel method for preparing palladium membranes by photocatalytic deposition, AIChE J. 46 (2000) 1075–1083.
[40] D. Fort, J.P.G. Farr, I.R. Harris, A comparison of palladium-silver and palladium-yttrium alloys as hydrogen separation membranes, J. Less Common Met. 39 (1975) 293–308.
[41] J.N. Keuler, L. Lorenzen, Developing a heating procedure to optimise hydrogen permeance through Pd–Ag membranes of thickness less than 2.2 μm, J. Membr. Sci. 195 (2002) 203–213.
[42] L. Yang, Z. Zhang, X. Gao, Y. Guo, B. Wang, O. Sakai, et al., Changes in hydrogen permeability and surface state of Pd–Ag/ceramic composite membranes after thermal treatment, J. Membr. Sci. 252 (2005) 145–154.
[43] L. Yang, Z. Zhang, B. Yao, X. Gao, H. Sakai, T. Takahashi, Hydrogen permeance and surface states of Pd–Ag/ceramic composite membranes, AIChE J. 52 (2006) 2783–2791.
[44] A.L. Mejdell, D. Chen, T.A. Peters, R. Bredesen, H.J. Venvik, The effect of heat treatment in air on CO inhibition of a ~3 μm Pd–Ag (23 wt%) membrane, J. Membr. Sci. 350 (2010) 371–377.
[45] T.A. Peters, M. Stange, R. Bredesen, On the high pressure performance of thin supported Pd–23%Ag membranes – evidence of ultrahigh hydrogen flux after air treatment, J. Membr. Sci. 378 (2011) 28–34.
[46] I.-H. Svenum, J.A. Herron, M. Mavrikakis, H.J. Venvik, Adsorbate-induced segregation in a PdAg membrane model system: Pd3Ag(111), Catal. Today 193 (2012) 111–119.
[47] H. Uchikawa, T. Okazaki, K. Sato, New technique of activating palladium surface for absorption of hydrogen or deuterium, Jpn. J. Appl. Phys. 32 (1993) 5095–5096.
[48] D. Wang, J.D. Clewley, T.B. Flanagan, R. Balasubramaniam, K.L. Shanahan, Enhanced rates of hydrogen absorption resulting from oxidation of Pd or internal oxidation of Pd–Al alloys, J. Alloys Compd. 298 (2000) 261–273.
[49] J.K. Ali, E.J. Newson, D.W.T. Rippin, Deactivation and regeneration of Pd–Ag membranes for dehydrogenation reactions, J. Membr. Sci. 89 (1994) 171–184.
[50] T.B. Flanagan, J.F. Lynch, J.D. Clewley, B. Von Turkovich, The effect of lattice defects on hydrogen solubility in palladium: I. Experimentally observed solubility enhancements and thermodynamics of absorption, J. Less Common Met. 49 (1976) 13–24.
[51] T. Mütschele, R. Kirchheim, Segregation and diffusion of hydrogen in grain boundaries of palladium, Scr. Metall. 21 (1987) 135–140.
[52] T. Mütschele, R. Kirchheim, Hydrogen as a probe for the average thickness of a grain boundary, Scr. Metall. 21 (1987) 1101–1104.
[53] G.J. Thomas, R.W. Siegel, J.A. Eastman, Grain boundaries in nanophase palladium: high resolution electron microscopy and image simulation, Scr. Metall. Mater. 24 (1990) 201–206.
[54] T.B. Flanagan, R. Balasubramaniarn, R. Kirchheim, Exploring lattice defects in palladium and its alloys using dissolved hydrogen, Part I: Hydrogen solubility and its segregation to dislocations and vacancies, Platin. Met. Rev. 45 (2001) 114–121.
[55] J.F. Lynch, J.D. Clewley, T. Curran, T.B. Flanagan, The effect of the α–β phase change on the α phase solubility of hydrogen in palladium, J. Less Common Met. 55 (1977) 153–163.
[56] H.C. Jamieson, G.C. Weatherly, F.D. Manchester, The β→α phase transformation in palladium–hydrogen alloys, J. Less Common Met. 50 (1976) 85–102.
[57] E. Ho, H.A. Goldberg, G.C. Weatherly, F.D. Manchester, An in situ electron microscope study of precipitation in palladium–hydrogen alloys, Acta Metall. 27 (1979) 841–853.
[58] W. Mekonnen, B. Arstad, H. Klette, J.C. Walmsley, R. Bredesen, H. Venvik, et al., Microstructural characterization of self-supported 1.6 μm Pd/Ag membranes, J. Membr. Sci. 310 (2008) 337–348.
[59] A. Bhargav, G.S. Jackson, Thermokinetic modeling and parameter estimation for hydrogen permeation through Pd0.77Ag0.23 membranes, Int. J. Hydrogen Energy 34 (2009) 5164–5173.
[60] X. Zhang, X.-H. Song, D.-L. Zhang, Thickness dependence of grain size and surface roughness for dc magnetron sputtered Au films, Chin. Phys. B 19 (2010) 086802.

[61] W.M. Tucho, R. Holmestad, J.C. Walmsley, NTNU, previously unpublished data.
[62] T.L. Ward, T. Dao, Model of hydrogen permeation behavior in palladium membranes, J. Membr. Sci. 153 (1999) 211–231.
[63] R. Dittmeyer, V. Höllein, K. Daub, Membrane reactors for hydrogenation and dehydrogenation processes based on supported palladium, J. Mol. Catal. A Chem. 173 (2001) 135–184.
[64] S. Uemiya, State of the art of supported metal membranes for gas separation, Sep. Purif. Rev. 28 (1999) 51–85.
[65] H. Hasegawa, K. Nakajima, Effect of hydrogen on the mechanical properties of Pd, J. Phys. F Met. Phys. 9 (1979) 1035–1046.
[66] H. Züchner, H.G. Schöneich, Improvement of electrochemical methods for studying the diffusion and solubility of hydrogen in metals, J. Less Common Met. 101 (1984) 363–372.
[67] Y. Li, Y.-T. Cheng, Hydrogen diffusion and solubility in palladium thin films, Int. J. Hydrogen Energy 21 (1996) 281–291.
[68] T.A. Peters, T. Kaleta, M. Stange, R. Bredesen, Development of thin binary and ternary Pd-based alloy membranes for use in hydrogen production, J. Membr. Sci. 383 (2011) 124–134.
[69] T.A. Peters, T. Kaleta, M. Stange, R. Bredesen, Hydrogen transport through a selection of thin Pd-alloy membranes: membrane stability, H_2S inhibition, and flux recovery in hydrogen and simulated WGS mixtures, Catal. Today 193 (2012) 8–19.
[70] T.A. Peters, T. Kaleta, M. Stange, R. Bredesen, Development of ternary Pd–Ag–TM alloy membranes with improved sulphur tolerance, J. Membr. Sci. 429 (2013) 448–458.